CERN/SPSC 98-17
SPSC/P308
July 13, 1998

PROPOSAL TO STUDY THE USE OF A CRYSTAL AS A 'QUARTER-WAVE PLATE' TO PRODUCE HIGH ENERGY CIRCULARLY POLARIZED PHOTONS

A. Apyan[a], R.O. Avakian[a], S. Ballestrero[b], C. Biino[c,d], P. Cenci[e], S.H. Connell[f], A. Gianoli[d], B. Gorini[d], K. Ispirian[a], P. Kasper[g], T. Ketel[h], Yu.V. Kononets[i,j], A. Lopez[k], S. Luitz[d], U. Mikkelsen[j,d], E. Menichetti[c], A. Perego[b], K. Piotrzkowski[l], J. Saborido[d], J.P.F. Sellschop[f], P. Sona[b], V. Strakhovenko[m], S. Trentalange[n], E. Uggerhøj[j*], M. Velasco[d*], Z.Z. Vilakazi[f]

[a]Institute of Physics, Yerevan, Armenia
[b]INFN and University of Firenze, Firenze, Italy
[c]INFN and University of Torino, Torino, Italy
[d]CERN, Geneva, Switzerland
[e]INFN, Perugia, Italy
[f]Schonland Research Centre, Johannesburg, South Africa
[g]Fermilab, Chicago, USA
[h]NIKHEF, Amsterdam, Netherlands
[i]Kurchatov Institute, Moscow, Russia
[j]Institute for Storage Ring Facilities, University of Aarhus, Denmark
[k]University of Santiago de Compostela, Santiago de Compostela, Spain
[l]DESY, Hamburg, Germany
[m]Institute of Nuclear Physics, Novosibirsk, Russia
[n]University of California, Los Angeles, USA
*Co-Spokespersons

Abstract

We present a proposal to study the use of a crystal as a 'quarter-wave plate' to produce high energy circularly polarized photons, starting from *unpolarized* electrons. The intention is to generate linearly polarized photons by letting electrons pass a crystalline target, where they interact coherently with the lattice nuclei. The photon polarization is subsequently turned into circular polarization after passing another crystal, which acts as a 'quarter-wave plate'.

1 Summary

The purpose of the proposed experiment is to study the use of a crystal as a 'quarter-wave plate' ($\lambda/4-$plate) to produce high energy circularly polarized photons, starting from *unpolarized* electrons.

It is possible to generate circularly polarized photons using a polarized electron beam, from either Compton scattering or using a crystalline material as a radiator. However, the currently available longitudinally polarized electron beams are of limited energy, ≤ 50 GeV.

We intend to study an alternative method in which one uses unpolarized electrons in a two-crystal setup. Electrons penetrating the first crystal generate the linearly polarized radiation. The polarization of these photons is 'rotated' in a second crystal, which acts as a $\lambda/4-$plate. By these means, higher energies and new physics opportunities will be possible with already existing beam facilities.

Some of the topics that can be addressed with a circularly polarized high energy photon beam are, for example, the polarized gluon contribution to the nucleon spin from polarized photo-production of jets and heavy quarks (produced via photon-gluon fusion) [1, 2, 3], and polarized photo-production of high transverse momentum mesons [4]. This topic is of great importance since the recent polarized deep inelastic scattering experiments[1)] have firmly established that only 30% of the nucleon spin is carried by quarks, as first observed by the EMC Collaboration [5]. Another example is the study of hidden strangeness in the nucleon. It was recently shown [6] that polarized photo-production of ϕ mesons is sensitive to this issue.

This experiment will take two weeks for setup, calibrations, and measurement of the linear polarization of the initial photon beam. The measurement of the circularly polarized radiation, generated when the linearly polarized photons traverse the $\lambda/4-$plate (second crystal) will require four extra weeks. In both cases, the polarization will be detected through the angular distributions of the π^+ π^- pairs resulting from ρ^0 photo-production in a Be target.

The necessary thickness of the $\lambda/4-$plate – and therefore the attenuation of the photon beam – decreases with increasing photon energy. For this reason we request a 180 GeV electron beam which will give a high yield of linearly polarized photons between 96-144 GeV. This choice is a compromise between beam intensity and the thickness for the $\lambda/4$-plate.

We request at least six weeks of beam time between the 1999 and 2000 CERN SPS run with the electron beam available in the H2 beam line in the North Area.

2 Theoretical background

2.1 Radiation of electron in crystals

Let us consider a charged particle penetrating a single crystal (Fig. 1 a). For sufficiently small angles of incidence to a crystallographic direction, the coherent scattering off the atomic constituents (Fig. 1 b) act on the particle as if the charges of the screened nuclei were smeared along this direction (Fig. 1 c). Thus, the particle is deflected by a 'continuous string of charge'. Even though the forces are purely electric in the laboratory frame, locally the deflection will have the same character as that of the deflection by a magnetic field. Furthermore, in the continuum approximation the field becomes of

[1)] The SMC Collaboration at CERN, the E142, E143, E154 and E155 Collaborations at SLAC, and the HERMES Collaboration at DESY.

macroscopic extension - all along the crystal.

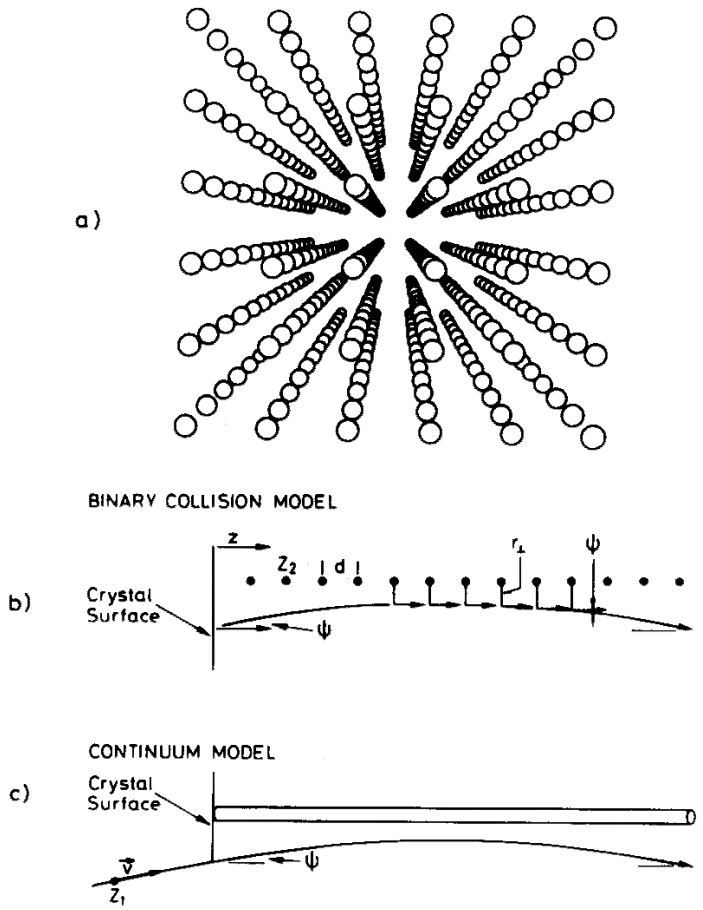

Figure 1: *a) Perspective view of the positions of individual atoms in a simple cubic lattice. Below, the deflection of an incident particle by a string of atoms in b) the binary collision picture and c) the continuum picture.*

The emission of synchrotron radiation by a charged particle passing a magnetic field is among other things characterized by the critical frequency, ω_c, beyond which the number of photons per frequency interval, $\mathrm{d}N/\mathrm{d}\omega$, decreases exponentially. The photon energy corresponding to this frequency is given by

$$\hbar\omega_c = 3\gamma EB/B_0, \tag{1}$$

where γ is the Lorentz factor, E the energy of the electron, B is the magnetic field and $B_0 = 4.4 \cdot 10^9$ T is the Schwinger field. Since the axial fields in a crystal correspond to magnetic fields of up to $\simeq 10^5$ T, a relativistic particle with $\gamma \simeq 10^5$ passing a crystal is likely to radiate a large fraction of its energy into one photon, according to Eq. (1). Calculated classically as above, it may even seem to radiate more energy than is available and thus quantum corrections become important for the calculation as pointed out by Schwinger [7]. The invariant parameter, $\chi = \gamma B/B_0$, is a measure of the quantum effects in synchrotron radiation and already when χ is around 0.1 the corrections become significant. This is the basis of the so-called strong field effects which have been investigated in detail by the NA43 collaboration at CERN led by Uggerhøj [8], and treated theoretically by several groups, e.g., the group led by Baier in Novosibirsk and Kononets in Moscow.

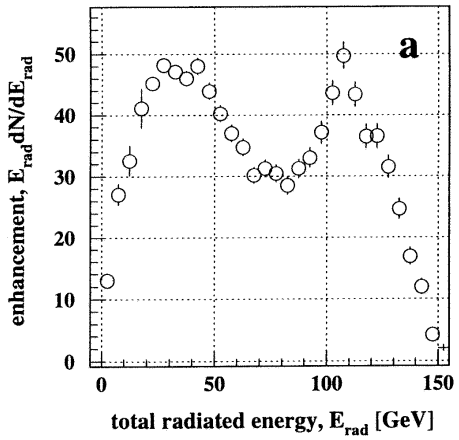

Figure 2: *Enhancement in channelling radiation with respect to Bethe-Heitler value. Radiation emitted by 150 GeV electrons penetrating a 0.7 mm diamond at 0.6 mrad off the* $\langle 110 \rangle$ *axis on the (111) plane.*

Another type of radiation obtained from the penetration of crystals is the more familiar 'coherent bremsstrahlung' (CB). This type of radiation has a maximum when the inverse formation length[2)] of the photon coincides with the projection of a vector of the reciprocal lattice on the direction of the electron. Equivalently, it is a resonance phenomenon which appears when the waves emitted from the passage of subsequent planes are in phase. Earlier studies, with the Omega spectrometer and a 80 GeV electron beam radiating off a Si-crystal, have shown that linear polarizations of 10-60% can be obtain with this method [9].

The two above mentioned phenomena can be combined in a single feature, the so-called Strings-Of-Strings (SOS) radiation. This appears in the intermediate region when the beam is incident in a plane, with a small angle to the axis. Here the influence from the strong field of the atomic strings of the axis affects the motion of a penetrating particle, in a way similar to the interaction with the planes in coherent bremsstrahlung. As a consequence, there will be two contributions: (1) Planar channelling radiation stemming from transitions between bound states in the transverse potential from the planes, and (2) radiation of the coherent type stemming from the periodic interaction with the atomic strings. These contributions appear as distinct features in a power-spectrum (Fig. 2) where the planar channelling radiation (1) appears at $\hbar\omega/E \simeq 0.2$ and the SOS radiation (2) peaks around $\hbar\omega/E \simeq 0.7$.

The average number of photons emitted by 150 GeV electrons passing a 0.7 mm diamond, aligned as for Fig. 2, is shown in Fig. 3c) . Note that the multiplicity is low, even though the effective radiation length is $\simeq 0.3X_0$. The composition of the produced photon beam was examined by converting the photons in the beam and analyzing them with a spectrometer, see Fig. 3 d). This shows that if the electron radiated more than 90 GeV, then the event is composed of a hard photons of $\simeq$ 100 GeV, followed by softer photons of $\leq$20 GeV.

Planar channelling radiation has been shown experimentally to be completely lin-

[2)] The formation length can be considered as the length over which the photon and the emitting electron become separated by one wavelength of the emitted radiation. In the case of pair creation, it is the length required to separate the e^+ and e^- by a Compton wavelength.

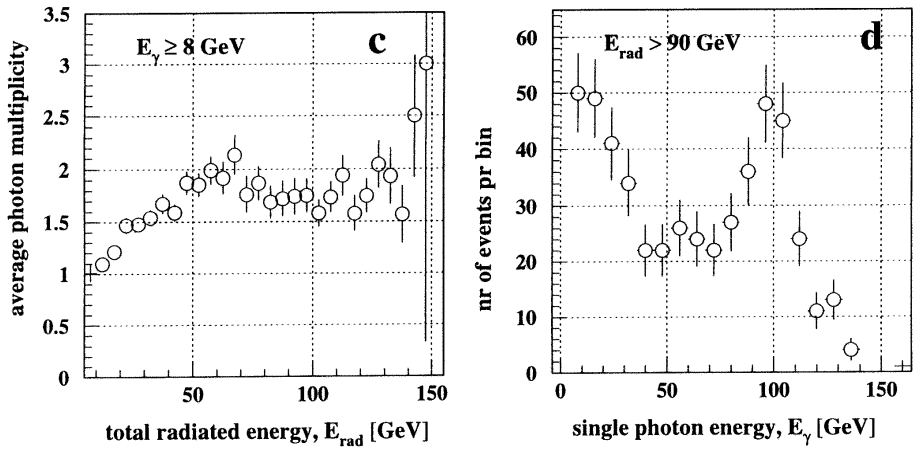

Figure 3: *c) The average number of photons emitted by 150 GeV electrons penetrating a 0.7mm diamond at 0.6 mrad off the* $\langle 110 \rangle$ *axis on the (111) plane. d) Counting spectrum of single photon events, where the electron has radiated 90 GeV or more in the same orientation as for c) (for details, see text).*

early polarized at lower energies [10]. This is to be expected, since in the rest frame of the longitudinal (along the planes) motion, the particle oscillates transversely as a dipole oscillator.

The SOS radiation behaves in many respects as the coherent bremsstrahlung. The important difference is that the SOS radiation is emitted while the particle is travelling between planes, subject to the strong axial fields, while in the CB case the particle is perturbed by the much weaker planar fields as it goes across planes. This has two consequences: the SOS radiation is harder, and is not 100% polarized as in planar channelling radiation. The NA43 experiment has shown that the emitted radiation is linearly polarized for unpolarized electrons incident in the SOS region (See Fig. 4), but the degree of polarization was not determined [3)]. Finally, the SOS radiation with respect to radiation from an amorphous material has an enhancement which is inversely proportional to the charge of the lattice nuclei apart from the dependence on lattice constants and density of scattering centres. This means that the enhancement is about a factor of 25 in Si instead of 40 as shown in Fig. 2 for diamond.

Similarly, pair production in the SOS-mode shows an enhancement (increase in yield by use of a crystal compared to an amorphous foil of the same thickness) that can be up to a factor 10 for the energies considered here, somewhat larger than for coherent pair production. It should be noted that this is comparable to the enhancement for radiation emission when averaged over all photon energies, ie. the decrease of the effective radiation length.

2.2 Birefringence: Quarter–wave plate capabilities of crystals

Already in the early sixties, it was proposed by Cabibbo and collaborators [12] to use a crystal as a $\lambda/4-$plate for energetic photons. This relies on the difference of the indices of refraction, n, for the photons polarized perpendicular and parallel to the crystallographic plane

$$\Re(n_\perp - n_\parallel)\hbar\omega \cdot x_{\lambda/4} = \pi/2, \tag{2}$$

[3)] A measurement of the linear polarization in SOS radiation is a part of our program.

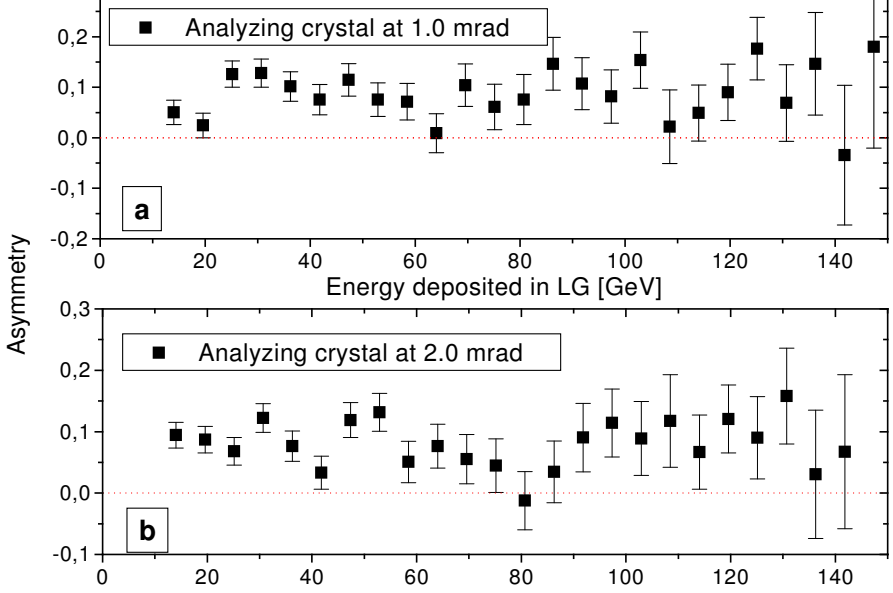

Figure 4: *Evidence of linear polarization in channelling radiation from the cross-section of e^+e^- pair production. Shown is the asymmetry, ie. the difference in pair production cross sections for photons polarized parallel to and perpendicular to the crystallographic plane, as a function of the energy radiated by the emitting electron.*

where $\hbar\omega$ is the photon energy and $x_{\lambda/4}$ the thickness of the $\lambda/4-$plate. At that time the effect was calculated with the theory of coherent pair production and bremsstrahlung. It was found that the photon beam would be attenuated severely due to the large crystal thickness required for a $\lambda/4$-plate.

Meanwhile, the above mentioned strong field effects, appearing at sufficiently high energy, have shown radiation and pair production spectra which are not describe by the theory of coherent bremsstrahlung or pair production. In particular, the predicted and observed enhancements of radiation (See Fig. 2) are about one order of magnitude higher than those calculated by coherent bremsstrahlung theory. This for example takes place in the Strings-Of-Strings (SOS) region, where the electron traverses the strings of atoms comprising the crystallographic axes. The photon multiplicity in this region is comparable to that of coherent bremsstrahlung [8]. The SOS radiation bears some resemblance to the traditional coherent radiation where the electron traverses the crystalline planes. The increase is due to the fact that the electric forces near an axis giving rise to the SOS radiation are about an order of magnitude higher than those near a plane, which are responsible for the traditional coherent radiation. It is expected that the birefringence effect, given by $\Re(n_\perp - n_\parallel)$, is a factor $\simeq$5 stronger for these crystallographic orientations and photon energies [13].

3 Proposed measurement

3.1 Polarization measurements of photons using ρ^0 photo-production

The linear and circular polarization of a photon beam can be measured from the $\pi^+\pi^-$ angular distribution of photo-produced ρ^0 vector mesons, $\gamma p \to \rho^0 p$. In the rest frame of the ρ^0:

$$\frac{\mathrm{dN}}{\mathrm{d}\cos\theta \mathrm{d}\phi} = W(\cos\theta,\phi)^0 + \sum_{\alpha=1}^{3} P_\gamma^\alpha W(\cos\theta,\phi)^\alpha, \qquad (3)$$

where the $W(\cos\theta, \phi)^i$ distributions are defined from the production amplitudes and the spin density matrices (see Ref. [15] for full description), and θ, ϕ are defined as the polar and the azimuthal angles with respect to one of the pions. The definition for the polarization vector, P_γ^α, depends on the kind of photon polarization:

$$\mathrm{P}_\gamma = \mathrm{P_L}(-\cos 2\Phi, -\sin 2\Phi, 0), \qquad \mathrm{P}_\gamma = \mathrm{P_C}(0, 0, \pm 1), \tag{4}$$

for linear and circular polarization, respectively, and where Φ is the angle between the γp production plane and the polarization vector of the photon. In this notation $\pm$ stand for right and left handed photons and $0 < (\mathrm{P_L},\ \mathrm{P_C}) < 1$. From Eq. (3)-(4) and under the assumption of s-channel helicity conservation, the linear and circular polarization of real photons can be found from:

$$\sigma_\mathrm{L} = \frac{3}{8}\{1 + \mathrm{P_L}\cos 2\psi\}, \tag{5}$$

$$\sigma_\mathrm{C} = \frac{3}{8}\{1 \pm \mathrm{P_C}\sin 2\phi\}, \tag{6}$$

where $\sigma_{\mathrm{L,C}}$ are the cross sections, and $\psi = \phi - \Phi$.

3.2 Beamline and tagging system

The beam requirements are fulfilled by the H2 beamline[17] for electron at 180 GeV, that is, low emittance and thus the possibility of an angular divergence of $\sim$50 μrad. Even though the beam intensity will be lower than at 150 GeV, the higher beam energies are desirable for the following reasons:

- The required thickness of the $\lambda/4$-plate is inversely proportional to the energy of the photon beam. Therefore a thinner crystal can be used, which will reduce the beam attenuation.
- The acceptance of the $\pi^+\pi^-$ pair of the decay ρ^0 is around 55% and 90% for ρ^0 of 50 and 100 GeV, respectively, in the proposed setup. This gain is without a significant change in the photo-production cross–section (See Fig. 5).
- The emittance of the beam decreases slightly as the energy is raised.

One drawback is that the characteristic angle for the SOS radiation decreases slowly with increasing energy, but it is only 10% smaller at 180 GeV compared to 150 GeV.

In order to have high beam intensity and reduce the data taking time to a minimum, we request:

- 5×10^{12} protons/pulse on T2.
- A production angle $\simeq$ 3.0 mrad[4)].
- more open beam collimation compared to the NA43 experiment. That is, a beam spot with $\oslash$ 40 mm instead of $\oslash$ 20 mm.

Under these conditions we should get 8×10^4 electrons/burst [11].

[4)] This is different from the standard 4.5 mrad and imposes certain restrictions on the choice of particles and momenta in the neighbouring H4 beamline.

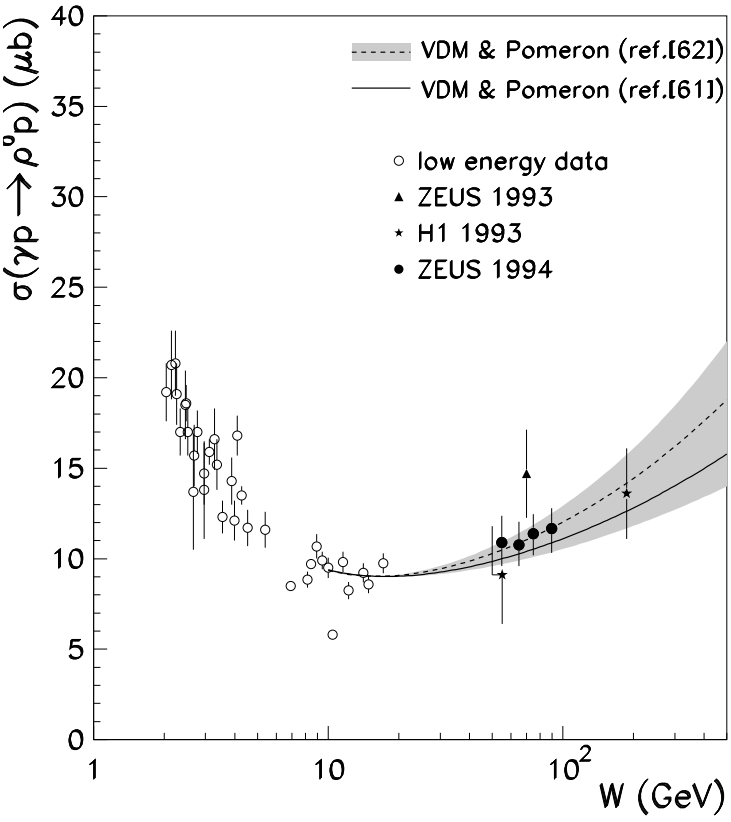

Figure 5: *Summary on data for ρ^0 photo-production cross-section [16] as a function of $W = \sqrt{2M_p E_\gamma}$, where M_p in the mass of the proton and E_γ the energy of the photon beam.*

The energy of the photons will be estimated in an event-by-event basis by tagging the incoming and outgoing electron. We are only interested in events where $E_\gamma/E_e \approx 0.7$ (SOS mode). The probability of emitting a second photon in the radiating crystal in the SOS mode is rather large. However, the typical energy of the extra photons is below 20 GeV which is a harmless change to the photon energy measurement since this information will only be used in the trigger, and the ρ^0 analysis will be based on the $\pi^+\pi^-$ momentum and vertex reconstruction.

The tagging system is defined by two 1 mm spacing proportional chambers (P1-2) located upstream of the B8 dipole magnet and one downstream (P3), as shown in Fig. 6. These chambers have been offered by the SL-division. The angular resolution for the electron track using the proposed positions for chambers P1 and P2 is $\sim 10\,\mu$rad. The typical angle for the emitted photon is rather small, $\theta = 1/\gamma$. As a consequence, both the impact point of the electron into the radiating-crystal, and the photon into the analyzing-crystal can be predicted precisely. The integrated field in B8 is $B \cdot l \simeq 4\,$Tm giving a total momentum resolution of $\delta p/p^2 \sim 0.0002\,\mathrm{GeV}^{-1}$.

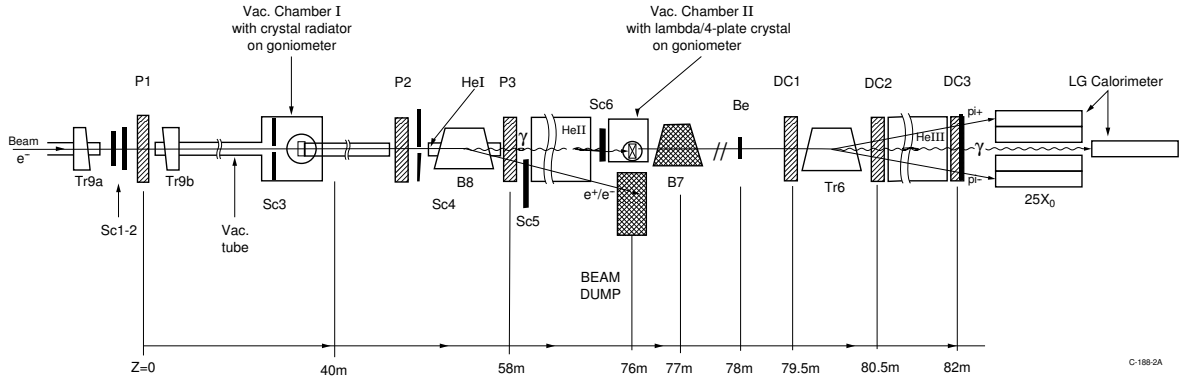

Figure 6: *Schematic drawing of the setup.*

3.3 Setup

A schematic drawing of the setup for the $\pi^+\pi^-$ detection is also shown in Fig. 6. For the linear polarization measurement we will need:

– $e^- \rightarrow (crystal_{rad}) \rightarrow (Be_{target}) \rightarrow \rho^0 \rightarrow \pi^+\pi^-$,

and for the circular polarization:

– $e^- \rightarrow (crystal_{rad}) \rightarrow (\lambda/4 - plate) \rightarrow (Be_{target}) \rightarrow \rho^0 \rightarrow \pi^+\pi^-$.

Therefore the setup will be the same for both measurements with the exception of the $\lambda/4$-plate.

The $\pi^+\pi^-$ spectrometer is defined by one drift chamber upstream of the Tr6 magnet and two downstream. The resolution of the chambers is $100\,\mu$m and the Tr6 magnet has a $B \cdot dl = 0.52$ Tm. The length of the Be-target used to photo-produce ρ^0 is limited to 5 cm in order to be able to use its position as a constraint in the vertex reconstruction. With this target length and the chosen chamber positions, the ρ^0 acceptance at 100 GeV is better than 90 %, and the average angle for a pion and its resolution is 0.005 ± 0.0001 rad. Similarly, the momentum resolution is $\delta p/p^2 < 0.0007$ GeV^{-1} , while the ρ^0 mass resolution is better than 0.02 GeV. Multiple scattering effects are dominated by the scattering in the Be target and are of the order of 70 μrad for a 50 GeV pion. A lead glass calorimeter (LG) will be used to reduce possible backgrounds due to γ conversion in the target, by discrimination of electromagnetic showers from hadronic ones. The chambers and the LG system have already been used by the NA43 collaboration and therefore known to have the required characteristics for the polarization measurements.

In the second setup, the $\lambda/4$-plate will also act as an unwanted target. Therefore, an extra 1.6 Tm magnet, B7, will be used to deflect some of the produced particles away from the Be-target.

The $\pi^+\pi^-$ trigger will be defined by the beam defining vetos (Sc1-6) anti coincidence with the electron tagging system and by a two track logic based on an array of hodoscopes located downstream of DC3. The hodoscope array has been taken from the beam hodoscope system of the NA47 experiment and will be modified and tested later this summer.

To achieve high performance and reliability while keeping the cost low, we propose to use standard CAMAC modules as front-ends and a PC as data acquisition computer. In the presence of a suitable network infrastructure in the experimental area the data should be sent directly to the computer centre for permanent storage and further analysis.

Table 1: *Crystal thickness and photon angle of incidence.*

Usage	Crystal	Thickness (mm)	angle of incidence to $\langle 110 \rangle$ (mrad)	effective radiation length
Radiator	Si	4	$= 0.3$ mrad	~ 1
$\lambda/4$-plate (CB)	Si	100	1.5 mrad	~ 2
$\lambda/4$-plate (SOS)	Si	44	$\simeq 0.7$ mrad	~ 2

The front end modules will be LeCroy FERA ADCs and TDCs housed in a CAMAC crate. The FERA modules offer 16 channels per module, short conversion times, built-in zero suppression and a high-speed ECL readout bus ("FERA Bus") on the front panel. A similar setup will be used for the PCOS2 system needed for the readout of the proportional chambers.

If required, other CAMAC modules like scalers or IO-registers can be easily added.

The CAMAC crate will be controlled by the PC via a PCI-CAMAC interface. To overcome the data rate limitations of CAMAC, it is planned to read out the modules via the front panel bus directly into the PC. A suitable interface has been developed by the NA48 collaboration (DT16 -to- S-Link -to- PCI interface) and is currently being used in their PC-based read-out system.

The PC houses the PCI-CAMAC and the DT16 interface as well as the disk buffer for intermediate data storage. A PentiumII-class machine does provide plenty of computing power for readout, online monitoring and data transport at the maximum sustained data rates of 1 Mbyte/s. To be able to make use of software (drivers, etc.) and knowledge existing in the NA48 collaboration we plan to use Linus as operating system.

To send the data to the computer centre, a single 100MBit/s Ethernet connection to the north area high speed network infrastructure would be sufficient. The buffering and data transfer scheme could be taken from the NA48 experiment.

As described above, most of the setup is available including detectors, readout and DAQ. This is the case since they have been used in previous experiments by members of this collaboration (NA43, NA47, NA48). The missing items will be rented from the pool (crates, power supplies, etc.), with the exception of the equipment needed for the modification of one of the two goniometers.

3.4 Crystals and target

This section gives some of the details for the crystals and targets to be used (See Table 1). Two estimates for the best $\lambda/4$-plate candidate are given. One operating in the CB mode and the other one in SOS. Due to the complexity of the calculations we are studying both options.

3.4.1 Radiator:

We will use a crystal radiator with a thickness of ~ 1 effective radiation length. This will give us a relatively low photon multiplicity and a reasonable rate of photon emission. A crystal of very low mosaic spread is needed, which limits us to choose between diamond, Si or Ge. Diamonds are not yet available in the required sizes, but is under investigation as described below. Ge is not our first choice, since the SOS radiation is not as well established as for Si. We will use 4 mm of Si $\langle 110 \rangle$. This corresponds to a radiation probability of 22%

for energy loss between 96 and 144 GeV by a 180 GeV incident electron. The 'SOS-peak' is more pronounced for angles to the plane smaller than the characteristic angle $\psi_c \simeq 20$ μrad, which takes about 30% of the phase-space of the beam. Outside this angular region the enhancement decreases by about a factor 2 for the angles of interest here, but the polarization is expected to be affected only outside $\simeq 3$ times ψ_c, ie. effectively outside the main part of the beam. This means that an overall efficiency factor of 0.7 should be included to take into account the angular dependence in the production of polarized photons. The expected total beam polarization for photons with energies between 96-144 is expected to be at least 50% in the SOS mode.

It would seem to be an attractive consideration to use diamond, which is superior to silicon as a radiator because the enhancement in the SOS region is almost a factor of two larger. The question necessarily arises as to the attainable size. Our Schonland colleagues have experience in the production of composite diamond targets : they have made two targets, each consisting of 16 diamonds of identical size and orientation, which they have arranged in a 4 by 4 matrix. Each diamond tile was 5 mm by 5 mm by 1 mm thick. The mutual alignment of these tiles is 170 μrad, and an investigation will be carried out as to how much better the alignment can be made in order to be useful for our purpose.

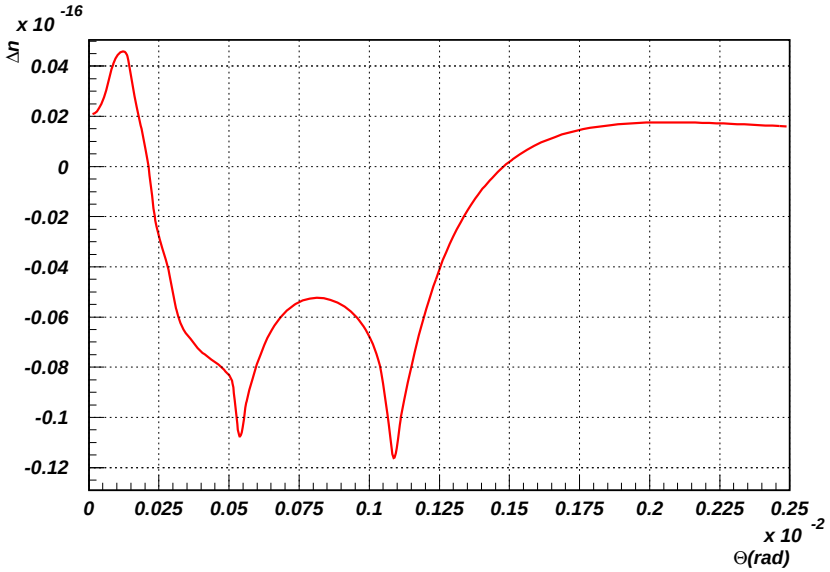

Figure 7: *Estimated* $\Delta n = \Re(n_{\|} - n_{\perp})$ *at room temperature as a function of the angle of incidence into a* $\langle 110 \rangle$ *Si crystal.*

3.4.2 $\lambda/4$*-plate:*

As explained in section 2.2, the 'goodness' of a crystal as a $\lambda/4$-plate depends on its birefringence capabilities. This is determined from its $\Re(n_{\|} - n_{\perp})$ where the indices of refraction $n_{\|}$ and $n_{\perp}$ correspond to the component seen by photons with parallel and perpendicular polarization with respect to the crystallographic plane. The optimal results for the crystal thickness, the photon angle of incidence and attenuation are given in Table 1 for crystal orientations where we are dominated either by CB or by SOS radiation effects. The calculations are based on the methods of Ref.[12] in the case of CB and on the recent SOS results of Ref.[13]. In both cases we are assuming an average photon energy of 150 GeV.

All numbers are summarized in Table 2, where we have defined the figure of merit (FMO) as $\epsilon_c\sqrt{N}$, where ϵ_c is the degree of circular polarization (assuming a 100% linearly polarized incident photon beam) and N is the number of surviving events out of 100 after taking into account the attenuation.

Estimates from coherent theory:
Figure 7 shows the $\lambda/4$-plate efficiency as a function of the thickness of a $\langle 110\rangle$ Si crystal at room temperature. As shown in Fig. 7, the optimal value of $\Re(n_{\parallel} - n_{\perp})$ is 1.15×10^{-17} for an angle of incidence of 1.1 mrad[5)]. This corresponds to a thickness of about 180 mm. The maximum production of circular polarization is limited to about 80% (see Fig.8). However, in order to reduce the beam attenuation we prefer to use a 100 mm crystal where the efficiency is about 70%, so that for 50% input linear polarization one still gets about 35% circular polarization. The beam attenuation will be about a factor of five.

Estimates from SOS theory:
Very recent results [13] have been obtained for the case of Si and Ge crystals in the SOS-mode.

For a 92 mm thick Si $\langle 110\rangle$ crystal at room temperature, aligned 0.7 mrad off the axis on the (100), plane one can obtain a 'true' $\lambda/4$-plate. That is, a 100% degree of circular polarization for an incident photon beam that is originally 100% linearly polarized. However, this will reduce the photon beam severely, such that only 1.6% of the photons remain. Instead, one may choose to reduce the degree of rotation into circular polarization to 38% by reducing the crystal thickness to 22.1 mm, but leads to a reduction of the photon beam intensity by to 63%. The optimum value for the FOM corresponds to a crystal thickness of 2L, where L=22.1 mm=attenuation length. This choice results in a 70% rotation efficiency.

For a Ge $\langle 110\rangle$ crystal at 100 K (with a weak deterioration expected when the temperature is raised to room temperature) aligned 0.5 mrad off the axis on the (100) plane, one obtains a $\lambda/4$-plate for a 20 mm thick crystal which leaves 1.4% of the photons 100% circularly polarized. The number of circularly polarized photons is maximized for the thickness 4.8 mm where again 37% of the photons survive, with a degree of circular polarization of 37%.

All these numbers are summarized in Table 2.

3.4.3 Be target:

A target length of 5 cm has been chosen as a compromise between ρ^0 event yield, multiple scattering of the $\pi^+\pi^-$ pair and the vertex resolution. This corresponds to 14% and 12.5% of radiation and interaction length, respectively. The cross section for $\gamma p \to \rho^0 p$ is $\sim 10\,\mu$barn in the useful photon energy range. Therefore, we expect $\sim 5 \times 10^{-6}$ photoproduced ρ^0 per incoming photon.

[5)] It must be noted, however, that according to the theory of strong field effects the usage of coherent theory becomes imprecise/erroneous when the angle of incidence becomes comparable to or smaller than about twice the so-called Baier angle, $\Theta = U/mc^2$ [14]. Here, U denotes the height of the transverse potential which leads to $\Theta \simeq 0.3$ mrad for the $\langle 110\rangle$ axis in Si.

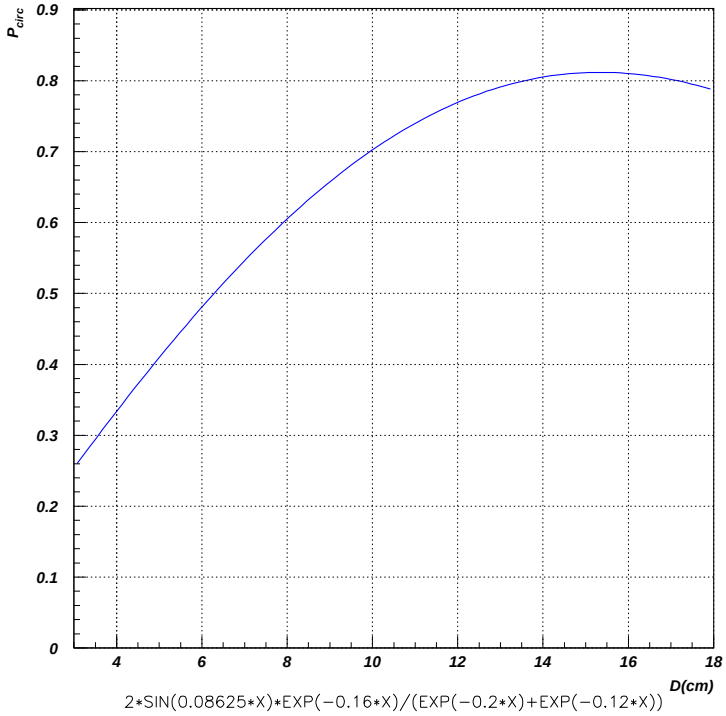

Figure 8: *Expected circular polarization of photons as a function of the Si crystal thickness (cm). It is assumed that the incoming polarization of the linearly polarized photon is 100%. The maximum transformation of circular polarization occurs for a 15 cm thick crystal, but we have chosen 10 cm as a compromise between polarization efficiency and beam attenuation.*

Table 2: *Summary of calculated values in % for different crystals and thicknesses for (quasi-) $\lambda/4$-plates in the SOS mode [13]. The figure of merit (FOM) is defined as $\epsilon_c\sqrt{N}$, where ϵ_c is the degree of circular polarization (assuming a 100% linearly polarized incident photon beam) and N is the number of surviving events out of 100 after taking into account the attenuation. (*) This value was optimized for a maximum number of photons.*

Crystal (thickness, mm)	Circular polarization	fraction of surviving photons	Figure of merit
SOS $\lambda/4$-plate			
Si $\langle 110\rangle$, (91.6)	100	1.57	1.3
Si $\langle 110\rangle$, (22.1)*	37.8	36.8	2.3
Si $\langle 110\rangle$, (44.2)	70	13.5	2.6
Ge $\langle 110\rangle$, (20.0)	100	1.41	1.2
Ge $\langle 110\rangle$, (4.8)*	36.8	36.8	2.2
Ge $\langle 110\rangle$, (9.6)	70	13.5	2.6
CB $\lambda/4$-plate			
Si $\langle 110\rangle$, (100.0)	70	20	3.1

4 Event yields and beam time request

The first step of this experiment will be to measure the linear polarization of the initial photon beam. This should be at least a 10% measurement since its uncertainty will enter as a systematic error in the second step, where the $\lambda/4$-plate is added and will transform only part of the linearly polarized photons into circular ones, and will act as a polarizer as well.

A data sample of a 1000 ρ^0 will give a statistical error on $\Delta P/P$ between 0.2-0.03 depending on the photon linear polarization. We have assumed that the polarization will be between 20-80% in these estimates.

Using the proposed radiator, we expect to have 1.5×10^6 photons per hour with energies between 96 and 144 GeV starting from 180 GeV electrons in the H2 beamline. This is after taking into account the requested electron beam intensity, a 22% radiation probability in the useful energy range, a 50% beam availability and a 70% beam angular acceptance. This means that we will have about 180 ρ^0 per day, and therefore at least a full week of data taking has to be taken assuming that the polarization is between 50-80%.

For the $\lambda/4$-plate we will choose a crystal thickness that will transform the polarization for at least 35-70% of the surviving photons. This is a compromise between $\lambda/4$-plate efficiency, accuracy of the polarization measurement and beam attenuation that can be as large as a factor of five. The expected accuracy on the measured linear and circular polarization can not be given apriori, since they depend on the absolute value of the polarization and efficiency of the $\lambda/4$-plate. However, in Table 3 we give several possibilities for the SOS and CB mode were we expected the $\lambda/4$-plate efficiency to be 37.8% and 70%, respectively. We can see that 4 weeks are needed to measure the circular polarization.

The time estimates assume that only one of the proposed $\lambda/4$-plate candidates will be tested. Since different phenomena are used in the two cases, that is, coherent bremsstrahlung (CB) versus strings-of-strings (SOS), it will be desirable to study both. Following the outcome of the cross checks for the calculations for the efficiency of the $\lambda/4$-plate in the two modes, we will decide whether to use CB or SOS first.

In summary, at least six weeks will be required to have the first study for using a Si crystal as a $\lambda/4$-plate. The data taking can be split in two parts 1999-2000, but enough time should be given in 1999 to have better understanding of the $\lambda/4$-plate before 2000. For this reason we request 4 weeks at the beginning of the 1999 SPS run. In addition to the installation and removal of the experiment apparatus, at least one full day each is needed to change the layout of beam elements forth and back as required.

References

[1] A.D. Watson, Z. Phys. C **12**, 123 (1982).
[2] M. Glück, E. Reya, Z. Phys. C **39**, 569 (1988).
[3] S. Keller, J.F. Owens, Phys. Rev. D **49**, 1199 (1994).
[4] A. Afanasev, C.E. Carlson and C. Wahlquist, hep-ph/9706522 (April, 1998).
[5] EMC, J. Ashman *et al.*, Phys. Lett. **B206**, 364 (1988); Nucl. Phys. **B328**, 1 (1989).
[6] A.I. Titov, *et. al.*, nucl-th/9804043.
[7] J. Schwinger, Phys. Rev. **75**, 1912 (1949).
[8] K. Kirsebom *et al.*, Nucl. Instr. Meth. B **119**, 79 (1996).
[9] P.J. Bussey *et al.*, Nucl. Instr. Meth. **211**, 301-308 (1983).
[10] M. Rzepka *et al.*, Nucl. Instr. Meth. B **90**, 186 (1994).
[11] N. Doble, private communication.
[12] N. Cabibbo, *et. al.*, Phys. Rev. Lett. **9**, 435 (1962).

Table 3: *Summary of expected statistical error in the polarization measurements for several polarization and efficiencies.*

Linear polarization $P_{\rm L}$	$\delta P_{\rm L}/P_{\rm L}$ 1000 ρ^0 ($180\rho^0$/day)	Efficiency:Attenuation of $\lambda/4$-plate	$P_{\rm C}$: $\delta P_{\rm C}/P_{\rm C}$ 1000 ρ^0 ($180\rho^0$/day)$\times$(attenuation)	Events needed for $\delta P_{\rm C}/P_{\rm C}$=0.05
SOS $\lambda/4$-plate				
20%	0.17	70%: 13.5/100	0.14: 0.22	>7000
50%	0.07	70%: 13.5/100	0.35: 0.08	$\sim$2000
80%	0.03	70%: 13.5/100	0.56: 0.05	$\sim$1000
CB $\lambda/4$-plate				
20%	0.17	70%: 20/100	0.14: 0.22	>7000
50%	0.07	70%: 20/100	0.35: 0.08	$\sim$2000
80%	0.03	70%: 20/100	0.56: 0.05	$\sim$1000

[13] Yu. Kononets, private communication.
[14] V.N. Baier, V.M. Katkov and V.M. Strakhovenko, Sov. Phys. Usp. **32**, 972 (1989).
[15] K. Schilling, P. Seyboth and G. Wolf, Nucl. Phys. **B15**, 397 (1970).
[16] ZEUS, hep-ex/97812020.
[17] H.W. Atherton, P. Coet, N. Doble, D.E. Plane, CERN/SPS 85-43.